



## Simple synthesis of layered H-octosilicate in situ surface-modified with lecithin

メタデータ	言語: en 出版者: Elsevier 公開日: 2021-02-16 キーワード (Ja): キーワード (En): Layered octosilicate, Soybean lecithin, pH control, Hydrothermal synthesis, Surface modification 作成者: Iwasaki, Tomohiro, Yamanaka, Yuki メールアドレス: 所属:
URL	<a href="http://hdl.handle.net/10466/00017227">http://hdl.handle.net/10466/00017227</a>

# 1 **Simple synthesis of layered H-octosilicate in situ surface-modified with lecithin**

2  
3 Tomohiro Iwasaki\*, Yuki Yamanaka

4 Department of Chemical Engineering, Osaka Prefecture University

5 1-1 Gakuen-cho, Naka-ku, Sakai, Osaka 599-8531, Japan

6 \* Corresponding author. iwasaki@chemeng.osakafu-u.ac.jp

## 7 8 **Abstract**

9 A simple process to synthesize H-octosilicate that is coated with a biocompatible natural  
10 surfactant lecithin has been developed, where the hydrothermal synthesis of Na-octosilicate,  
11 ion exchange of sodium ions in Na-octosilicate with protons, and surface modification with  
12 hydrogenated soy lecithin are sequentially performed in an identical reactor vessel. In the  
13 hydrothermal process, the solution pH was appropriately controlled according to a specific pH  
14 adjustment procedure, which successfully achieved a high yield (91% in 72 h) of Na-  
15 octosilicate. This high yield enabled the conversion of Na-octosilicate to H-octosilicate in the  
16 slurry through an acid treatment with no additional operations to remove the unreacted silicate  
17 species, such as washing and solid-liquid separation. Subsequently, the addition of a lecithin  
18 solution to the H-octosilicate slurry resulted in the formation of lecithin-coated H-octosilicate  
19 in situ. The final product (organo-octosilicate) was characterized through XRD, FT-IR, TG-  
20 DTA and SEM analyses, which confirmed that it maintained original shapes after the treatments,  
21 and lecithin was adsorbed on the surface of H-octosilicate with a mass ratio of approximately  
22 0.24 g-lecithin/g-H-octosilicate. An aqueous suspension of lecithin-coated H-octosilicate  
23 showed good dispersion under neutral conditions according to the pH dependence of the zeta  
24 potential. In addition, the surface modification inhibited their aggregation even under dry  
25 conditions. The results suggest that the developed process contributes to an industrial  
26 production of surfactant-coated H-octosilicate.

## 27 28 **Keywords:**

29 Layered octosilicate, Soybean lecithin, pH control, Hydrothermal synthesis, Surface  
30 modification

## 31 32 **1. Introduction**

33 Layered silicates are promising materials to synthesize various functionalized materials,

34 such as composites with inorganic and/or organic compounds and organo-silicate nanosheets,  
35 due to their peculiar structure (Attar et al., 2019; Carniato et al., 2020; Doustkhah and Ide, 2019;  
36 Funes et al., 2020; Ge et al., 2019; Mokhtar et al., 2020; Ryu et al., 2020; Selvam et al., 2014;  
37 Sirinakorn et al., 2018; Takahashi and Kuroda, 2011; Wang et al., 2019; Yuan et al., 2019).  
38 Octosilicate (also called as ilerite or RUB-18 and denoted as Na-octosilicate hereafter) (Iler,  
39 1964; Vortmann et al., 1997), which is a layered alkali polysilicate, has unique morphologies,  
40 i.e., thin, flat and regular rectangular plate-like shapes and smooth surfaces. In addition, the  
41 lateral size is controllable in the synthesis (Iwasaki et al., 2006). Therefore, octosilicate has  
42 been used to develop various high-performance composites (Asakura et al., 2019; Selvam et al.,  
43 2014; Sirinakorn et al., 2018; Sohmiya et al., 2018; Takahashi and Kuroda, 2011). Furthermore,  
44 H-octosilicate, which is obtained via ion exchange of Na<sup>+</sup> ions in the interlayers and surfaces  
45 of Na-octosilicate with H<sup>+</sup> ions, has attracted attention because it has silanol groups, which can  
46 be used for various chemical reactions due to their reactivity, in the interlayers and on surfaces,  
47 and it has no intercalate water (Borowski et al., 2002; Iwasaki, 2020; Iwasaki et al., 2000; Kiba  
48 et al., 2010; Kosuge and Singh, 2000; MacEdo and Airoidi, 2009; Nishimura et al., 2010;  
49 Nishimura and Inoue, 2014).

50 In many practical applications of Na- and H-octosilicates, the particles are desired to  
51 disperse without aggregation to sufficiently express their properties; however, the particles  
52 prepared by conventional synthesis processes tend to form aggregates. In particular, H-  
53 octosilicate particles often strongly aggregate due to the hydrogen bonds between silanol groups  
54 on the surfaces. Accordingly, the surface modification is required to reduce the aggregation.  
55 Many researchers have modified the surface of Na-octosilicate via ion exchange of Na<sup>+</sup> ions  
56 with organic cations (Ide et al., 2011; Nakamura and Ogawa, 2012). In contrast, to the best our  
57 knowledge, no paper focused on the surface modification of H-octosilicate; therefore, it is still  
58 a challenging research problem.

59 In conventional hydrothermal syntheses of Na-octosilicate using a sodium silicate solution,  
60 the formation reactions reach equilibrium at above 10 days and the yield (conversion) at  
61 equilibrium is approximately 40% (Iwasaki et al., 2006). Accordingly, large amounts of reactant  
62 (colloidal silicate species) remain in the solution. In the conversion of Na-octosilicate to H-  
63 octosilicate via an acid treatment for the ion exchange, when the Na-octosilicate suspension  
64 before adding the acid solution contains colloidal silicate species, the acid addition may result  
65 in deposition of amorphous silicates on the surface of Na-octosilicate, which remain as  
66 contaminants in the final H-octosilicate. Thus, in the conventional processes, prior to the ion

67 exchange and subsequent surface modification, the synthesized particles must be thoroughly  
68 washed to remove the unreactants, followed by solid-liquid separation; this is a crucial issue in  
69 the industrial production of surface-modified H-octosilicates since the complicated processes  
70 with multiple operations can increase the production cost and environmental impact. Therefore,  
71 simple processes without such additional operations are required for the industrial production.

72 To avoid additional operations, the promotion of the reactions, i.e., increase in the yield of  
73 Na-octosilicate, to reduce the concentrations of unreactants in the hydrothermal process is  
74 effective, which can be performed by decreasing the solution pH in the process, because the  
75 concentration of hydroxide ions in the solution increases as the hydrothermal formation of Na-  
76 octosilicate proceeds (Iwasaki et al., 2007). This decrease may enable the ion exchange and  
77 surface modification using simple conventional methods after the hydrothermal synthesis  
78 without the postwashing and postseparation operations. This study aims to develop a simple  
79 process using the pH control technique to in situ synthesize surface-modified H-octosilicate.  
80 Namely, the novelty of the study is that a series of treatments, i.e., hydrothermal synthesis, ion  
81 exchange and surface modification, is performed in an identical reactor vessel by sequentially  
82 adding an acid solution and a surface modifier to the solution after the hydrothermal process.  
83 As a surface modifier, biocompatible natural surfactant lecithin was used as a model surfactant  
84 (Fernández et al., 2020; Merino et al., 2016). The lecithin-coated H-octosilicate is promising  
85 ingredients in possible applications such as cosmetics (Iwanaga et al., 2020) and paints  
86 (Fernández et al., 2020) which require not only high dispersibility in water but also high safety.  
87 The aggregation-inhibition effects of the surface modification with lecithin was investigated.

88

## 89 **2. Experimental**

### 90 *2.1. pH-controlled synthesis of Na-octosilicate*

91 Na-octosilicate was hydrothermally synthesized in the presence of seed crystals according  
92 to our method (Iwasaki et al., 2006). The seed crystals were prepared in advance by the  
93 hydrothermal treatment of a sodium silicate solution (Nippon Chemical Industrial; SiO<sub>2</sub>: 23.44  
94 mass%, Na<sub>2</sub>O: 6.29 mass%) at 110°C for 13 days using an autoclave in the absence of seed  
95 crystals and additives (Iwasaki et al., 2006; Iwasaki et al., 2012). Subsequently, the pH-  
96 controlled hydrothermal synthesis was conducted as follows. A predetermined amount of seed  
97 crystals was added to the sodium silicate solution, where the mass ratio of seed crystals to  
98 solution was 0.1, and the resulting suspension was heated in an autoclave at 110°C after the  
99 aggregates of seed crystals were disintegrated by ultrasonication (40 W, 20 kHz) for 2 min. The

100 initial pH value of the solution before heating was 11.5, and the pH gradually increased as the  
101 formation reactions of Na-octosilicate proceeded. After each predetermined heating time period,  
102 the solution was cooled to room temperature, and the pH was decreased to the initial value  
103 (11.5) by adding a proper amount of 1 mol/L HCl to the solution. Then, the solution was  
104 reheated, and the hydrothermal treatment was resumed. The time interval of the pH adjustment  
105 was 6 h, 12 h and 24 h in this work. To determine the yield of Na-octosilicate in the process,  
106 the resulting precipitate was centrifuged and washed with deionized water several times and  
107 dried at 40°C for 3 days in air under atmospheric pressure. The yield was defined as the mass  
108 ratio of the dried sample to the theoretical maximum amount of Na-octosilicate prepared using  
109 the starting solution.

110

## 111 *2.2. Synthesis of lecithin-modified H-octosilicate*

112 The surface modification of H-octosilicate with lecithin was sequentially performed after  
113 the ion exchange of Na<sup>+</sup> ions in Na-octosilicate with H<sup>+</sup> ions to convert Na-octosilicate into H-  
114 octosilicate without centrifugation and washing operations. In the ion exchange, a proper  
115 amount of 1 mol/L HCl was added at room temperature to the Na-octosilicate slurry obtained  
116 from the pH-controlled synthesis using an optimized procedure. The pH of the slurry was  
117 adjusted to 4.0. After 24 h, a predetermined amount of 0.4 mass% lecithin aqueous solution was  
118 added to the H-octosilicate slurry, and the lecithin-containing slurry was allowed to stand at  
119 room temperature for 24 h. In this work, a cosmetic-grade hydrogenated soybean lecithin was  
120 used, which was purchased from Pinoa (Japan). The mass ratio of lecithin to H-octosilicate in  
121 the slurry was 0.4. The surface-modified sample was obtained after the purification similar to  
122 the described posttreatments of the synthesis of seed crystals.

123

## 124 *2.3. Characterization*

125 X-ray diffraction (XRD) analysis was conducted for several samples to confirm the  
126 formation of Na- and H-octosilicates using a powder X-ray diffractometer (XRD-6100,  
127 Shimadzu) with CuK $\alpha$  radiation. The morphologies were observed with a scanning electron  
128 microscope (SEM; S-2150, Hitachi). The IR spectra were recorded on an FT-IR spectrometer  
129 (IRAffinity-1, Shimadzu) via the diffuse reflectance method. The zeta potential was measured  
130 via electrophoretic light scattering (Zetasizer Nano ZS, Malvern) for a dilute lecithin-coated H-  
131 octosilicate suspension, whose pH was changed by adding proper amounts of 1 mol/L HCl and  
132 1 mol/L NaOH solutions. The thermogravimetry-differential thermal analysis (TG-DTA) for

133 the lecithin-coated H-octosilicate was performed with a thermogravimetric analyzer (SDT 2960,  
134 TA Instruments) at a heating rate of 10°C/min in an argon flow (100 mL/min).

135

### 136 **3. Results and discussion**

#### 137 *3.1. pH-controlled synthesis*

138 A possible mechanism of hydrothermal formation of Na-octosilicate is illustrated in Scheme  
139 1. Na-octosilicate can be constructed via the formation of low-molecular silicate species (such  
140 as oligomers) with silanol groups by hydrolysis and subsequent condensation–polymerization  
141 (Iler, 1979). In the reaction process, hydroxide ions are generated by an acid–base equilibrium  
142 of silicate species, which increases the solution pH. At the same time, this can decrease the  
143 concentration of reactant silicate species with silanol groups according to the equilibrium. Thus,  
144 a decrease in pH by an acid addition is effective to promote the formation reactions of Na-  
145 octosilicate.

146 The pH variations in the hydrothermal process with various pH adjustment procedures are  
147 shown in Fig. 1. When the time interval of the pH adjustment was 6 h and 12 h, the pH was  
148 approximately below 12 during the process; however, when the pH was adjusted every 24 h, it  
149 reached 12 in the early stages before decreasing the pH, similar to the case without pH control.  
150 The yields of Na-octosilicate in 72 h for these cases are illustrated in Fig. 2. The pH control in  
151 the hydrothermal process drastically improved the yield; in particular, when the time interval  
152 was 6 h and 12 h, the yields exceeded 80%. The XRD analysis and SEM observation confirm  
153 the formation of Na-octosilicate in all cases (data not shown). The results demonstrate the  
154 effectiveness of the pH control in the Na-octosilicate production.

155 The variations in yield when the pH was adjusted every 12 h and that in the pH-uncontrolled  
156 synthesis are shown in Fig. 3. When the pH was controlled, the yield linearly increased with  
157 treatment time, whereas the pH-uncontrolled synthesis made the yield almost constant after 36  
158 h. However, even in the pH-controlled synthesis, the rate of increase in yield slightly decreased  
159 after 48 h, possibly due to a decrease in concentration of silicate species. To enhance the  
160 reactions, the pH was adjusted to 11.0 after 48 h. As shown in Fig. 4, the rate of increase in  
161 yield was improved even after 48 h, and the yield reached 91% in 72 h. The XRD analysis  
162 confirms the formation of a uniform phase of Na-octosilicate, as shown in Fig. 5a. In an  
163 additional experiment for a comparison, the pH was adjusted to 11.0 at early stages of the  
164 hydrothermal process; however, some silicate compounds deposited due to high concentrations  
165 of silicate species, which resulted in gelation. Accordingly, the hydrothermal process with the

166 appropriate pH control contributed to a high-yield production of Na-octosilicate.

167

### 168 3.2. Surface modification with lecithin

169 Using the described method, the Na-octosilicate slurry with a yield of 91% was prepared  
170 and cooled to room temperature. To convert Na-octosilicate into H-octosilicate, a proper  
171 amount of 1 mol/L HCl was directly added to the Na-octosilicate slurry in the reactor vessel.  
172 Although small amounts of unreacted silicate species remained in the slurry after the  
173 hydrothermal treatment, the HCl addition resulted in no deposition of silicate compounds. In  
174 contrast, when the HCl solution was added to a Na-octosilicate slurry with a yield of  
175 approximately 40%, which was obtained after 72 h of the pH-uncontrolled hydrothermal  
176 process (Fig. 3), the slurry gelled due to the deposition of silicates, and no following treatments  
177 could be performed. The results suggest that high yields of Na-octosilicate by the appropriate  
178 pH control are required to simply perform the ion exchange in an identical vessel.

179 Subsequently, the lecithin solution was added to the resulting H-octosilicate slurry for  
180 surface modification. The XRD patterns of Na-octosilicate and H-octosilicate before and after  
181 the surface modification with lecithin are shown in Fig. 5. The crystal structure of Na-  
182 octosilicate (identical to RUB-18) was analyzed by Vortmann et al. (1997); they proposed a  
183 possible model for the structure that the silicate layer is built up of the basic unit made of four  
184 five-membered rings containing eight  $\text{SiO}_4$  tetrahedra. According to the structure, they also  
185 determined the chemical formula of  $\text{Na}_8[\text{Si}_{132}\text{O}_{64}(\text{OH})_8] \cdot 32\text{H}_2\text{O}$ . Na-octosilicate has a basal  
186 spacing of 1.10 nm, and the ion exchange decreased the basal spacing to 0.73 nm, which shifted  
187 the diffraction peak of the (004) plane to a low-angle region. The change in the XRD patterns  
188 coincided with that reported in literature (Werthmann et al., 2000). H-octosilicate (identical to  
189 H-RUB-18) has a chemical formula of  $\text{Si}_4\text{O}_7(\text{OH})_2$  (Borowski et al., 2002). The XRD analysis  
190 confirms that the surface modification do not change the crystal structure of H-octosilicate  
191 because this surface modification was carried out at room temperature and the concentration of  
192 the lecithin solution was relatively low compared with those in the lecithin intercalation  
193 (Merino et al., 2016).

194 The IR spectrum of the lecithin-coated H-octosilicate are shown in Fig. 6 with those of bare  
195 H-octosilicate and lecithin. The bare H-octosilicate (Fig. 6b) showed absorption bands at  
196 approximately 944 and 805  $\text{cm}^{-1}$ , which are attributed to asymmetric stretching vibration of Si-  
197 OH and symmetric bending vibration of Si-O-Si, respectively. In addition, the absorption  
198 bands were observed at approximately 3628 and 3177  $\text{cm}^{-1}$ , indicating the presence of Si-OH

199 groups and water molecules. In contrast, the lecithin-coated H-octosilicate (Fig. 6c) also had  
200 absorption bands at approximately 2918 and 2851  $\text{cm}^{-1}$  (C–H stretching vibration of =CH<sub>2</sub>  
201 group), 1738  $\text{cm}^{-1}$  (C=O stretching vibration) and 1470  $\text{cm}^{-1}$  (C–H stretching vibration of –  
202 CH<sub>3</sub> group) (Meng et al., 2018; Merino et al., 2016), which well coincided with those in the  
203 spectrum of lecithin (Fig. 6a). Accordingly, the XRD and IR analyses confirmed that lecithin  
204 molecules were adsorbed on the H-octosilicate surfaces. Thus, the increase in yield of Na-  
205 octosilicate in the hydrothermal synthesis led to success of the surface modification using the  
206 simple process, whereas conventional hydrothermal processes do not allow to perform  
207 subsequent ion exchange and surface modification treatments due to low yields, resulting in  
208 complicating the production process of surface-modified H-octosilicate.

209 The TG and DTA curves shown in Fig. 7 confirm that the bare and lecithin-coated H-  
210 octosilicate contain small amounts of water and the thermal decomposition of lecithin occurs at  
211 temperatures above approximately 150°C. Accordingly, the lecithin content in the lecithin-  
212 coated H-octosilicate was calculated using the weight loss from 150°C to 600°C and determined  
213 as 0.24 g-lecithin/g-H-octosilicate. The SEM images of the bare and lecithin-coated H-  
214 octosilicate samples with the photographs of 1 mass% aqueous suspensions, which were  
215 ultrasonicated for 3 min and kept under static conditions for 2 h, are shown in Fig. 8. The bare  
216 H-octosilicate particles tended to aggregate, which resulted in a rapid sedimentation in water.  
217 In contrast, the lecithin-coated H-octosilicate particles were spontaneously well disintegrated  
218 and relatively stably dispersed in water. The pH dependence of the zeta potential of a dilute  
219 suspension of lecithin-coated H-octosilicate is shown in Fig. 9. In a pH range of 4–7, the  
220 suspensions had high zeta potential, which suggests a stable dispersion in the natural pH range  
221 due to steric hindrance and electrostatic repulsion among lecithin molecules adsorbed on the  
222 surface of H-octosilicate. The dispersibility of lecithin-coated H-octosilicate in aqueous  
223 solutions is expected to satisfy requirements for practical applications such as cosmetics and  
224 water-based paints.

225

#### 226 **4. Conclusions**

227 A simple process to synthesize the lecithin-coated H-octosilicate has been developed, which  
228 is constructed by a series of treatments (i.e., hydrothermal synthesis, ion exchange and surface  
229 modification) performed in an identical reactor vessel. In the hydrothermal synthesis of Na-  
230 octosilicate, an appropriate control of the pH of solution can achieve a high yield, which enables  
231 the post acid treatment to convert Na-octosilicate into H-octosilicate in the slurry with no

232 additional operations to remove the unreacted silicate species, followed by the in situ surface  
233 modification with hydrogenated soy lecithin. The surface modification inhibited the  
234 aggregation of the coated particles even under dry conditions. In addition, the lecithin-coated  
235 H-octosilicate exhibited good dispersion in an aqueous solution in a neutral pH range. The  
236 developed process can contribute to an industrial production of surface-modified H-octosilicate.

237

## 238 **References**

239 Asakura, Y., Sugihara, M., Hirohashi, T., Torimoto, A., Matsumoto, T., Koike, M., Kuroda, Y.,  
240 Wada, H., Shimojima, A., Kuroda, K., 2019. Formation of silicate nanoscrolls through  
241 solvothermal treatment of layered octosilicate intercalated with organoammonium ions.  
242 *Nanoscale* 11, 12924–12931.

243 Attar, K., Demey, H., Bouazza, D., Sastre, A.M., 2019. Sorption and desorption studies of Pb(II)  
244 and Ni(II) from aqueous solutions by a new composite based on alginate and magadiite  
245 materials. *Polymers* 11, 340.

246 Borowski, M., Marler, B., Gies, H., 2002. The crystal structure determination of the crystalline  
247 layered silicic acid H-RUB-18. *Z. Kristallogr.* 217, 233–241.

248 Carniato, F., Gatti, G., Bisio, C., 2020. An overview of the recent synthesis and  
249 functionalization methods of saponite clay. *New J. Chem.* 44, 9969–9980.

250 Doustkhah, E., Ide, Y., 2019. Bursting exfoliation of a microporous layered silicate to three-  
251 dimensionally meso-microporous nanosheets for improved molecular recognition. *ACS*  
252 *Appl. Nano Mater.* 2, 7513–7520.

253 Fernández, M.A., Barberia Roque, L., Gámez Espinosa, E., Deyá, C., Bellotti, N., 2020.  
254 Organo-montmorillonite with biogenic compounds to be applied in antifungal coatings.  
255 *Appl. Clay Sci.* 184, 105369.

256 Funes, I.G.A., Peralta, M.E., Pettinari, G.R., Carlos, L., Parolo, M.E., 2020. Facile modification  
257 of montmorillonite by intercalation and grafting: The study of the binding mechanisms of a  
258 quaternary alkylammonium surfactant. *Appl. Clay Sci.* 195, 105738.

259 Ge, M., Tang, W., Du, M., Liang, G., Hu, G., Jahangir Alam, S.M., 2019. Research on 5-  
260 fluorouracil as a drug carrier materials with its in vitro release properties on organic  
261 modified magadiite. *Eur. J. Pharm. Sci.* 130, 44–53.

262 Ide, Y., Iwasaki, S., Ogawa, M., 2011. Molecular recognition of 4-nonylphenol on a layered  
263 silicate modified with organic functionalities. *Langmuir* 27, 2522–2527.

264 Iler, R.K., 1964. Ion exchange properties of a crystalline hydrated silica. *J. Colloid Sc.* 19, 648–

265 657.

266 Iler, R.K., 1979. *The Chemistry of Silica: Solubility, Polymerization, Colloid and Surface*  
267 *Properties and Biochemistry of Silica*. Wiley-Interscience, New York.

268 Iwanaga, T., Nioh, A., Reed, N., Kiyokawa, H., Akatsuka, H., 2020. A novel water-in-oil  
269 emulsion with a lecithin-modified bentonite prevents skin damage from urban dust and  
270 cedar pollen. *Int. J. Cosmet. Sci.* 42, 229–236.

271 Iwasaki, T., 2020. Structure of a layered octosilicate intercalated with alkylamines with  
272 different molecular structures in water. *J. Solid State Chem.* 290, 121545.

273 Iwasaki, T., Satoh, M., Masuda, T., Fujita, T., 2000. Powder design for UV-attenuating agent  
274 with high transparency for visible light. *J. Mater. Sci.* 35, 4025–4029.

275 Iwasaki, T., Kuroda, T., Ichio, S., Satoh, M., Fujita, T., 2006. Seeding effect on crystal growth  
276 in hydrothermal synthesis of layered octosilicate. *Chem. Eng. Commun.* 193, 69–76.

277 Iwasaki, T., Murai, K., Watano, S., 2007. Crystal growth mechanism of layered octosilicate  
278 ilerite in the hydrothermal synthesis. *J. Soc. Powder Technol., Japan* 44, 434–440 (in  
279 Japanese).

280 Iwasaki, T., Matsuyama, A., Nakamura, H., Watano, S., 2012. Rapid synthesis of octosilicate,  
281 a layered alkali silicate, by heterogeneous nucleation at the solid-liquid interface. *Appl. Clay*  
282 *Sci.* 58, 39–43.

283 Kiba, S., Itagaki, T., Nakato, T., Kuroda, K., 2010. Interlayer modification of a layered H-  
284 octosilicate (H-RUB-18) with methanol: formation of a highly ordered organosilicate  
285 nanohybrid. *J. Mater. Chem.* 20, 3202–3210.

286 Kosuge, K., Singh, P.S., 2000. Mixed-oxide pillared silicates from H-ilerite by intercalation.  
287 *Chem. Mater.* 12, 421–427.

288 MacEdo, T.R., Airoidi, C., 2009. New inorganic-organic lamellar derivatives synthesized from  
289 H-RUB-18 and thermodynamics of cation sorption. *New J. Chem.* 33, 2081–2089.

290 Meng, N., Chu, X., Ge, M.Q., Zhang, M., Sun, B., Su, Y.-T., Zhou, N.-L., 2018. Preparation  
291 and characterization of lecithin–heparin intercalated in montmorillonite nanocomposite.  
292 *Appl. Clay Sci.* 162, 454–460.

293 Merino, D., Ollier, R., Lanfranconi, M., Alvarez, V., 2016. Preparation and characterization of  
294 soy lecithin-modified bentonites. *Appl. Clay Sci.* 127–128, 17–22.

295 Mokhtar, A., Abdelkrim, S., Djelad, A., Sardi, A., Boukoussa, B., Sassi, M., Bengueddach, A.,  
296 2020. Adsorption behavior of cationic and anionic dyes on magadiite-chitosan composite  
297 beads. *Carbohydr. Polym.* 229, 115399.

298 Nakamura, T., Ogawa, M., 2012. Attachment of the sulfonic acid group in the interlayer space  
299 of a layered alkali silicate, octosilicate. *Langmuir* 28, 7505–7511.

300 Nishimura, S., Matsumura, H., Kosuge, K., Yamaguchi, T., 2010. Electric response of  
301 nonspherical and spherical silica particle dispersions to Ac electric field. *Langmuir* 26,  
302 10357–10364.

303 Nishimura, S., Inoue, T., 2014. Electro-optics of plate-like silica particle suspension. *Colloid.*  
304 *Surface. A* 440, 175–184.

305 Ryu, H.-J., Hang, N.T., Lee, J.-H., Choi, J.Y., Choi, G., Choy, J.-H., 2020. Effect of organo-  
306 smectite clays on the mechanical properties and thermal stability of EVA nanocomposites.  
307 *Appl. Clay Sci.* 196, 105750.

308 Selvam, T., Inayat, A., Schwieger, W., 2014. Reactivity and applications of layered silicates and  
309 layered double hydroxides. *Dalton Trans.* 43, 10365–10387.

310 Sirinakorn, T., Imwiset, K., Bureekaew, S., Ogawa, M., 2018. Inorganic modification of layered  
311 silicates toward functional inorganic-inorganic hybrids. *Appl. Clay Sci.* 153, 187–197.

312 Sohmiya, M., Nakamura, T., Sugahara, Y., Ogawa, M., 2018. Distribution control-oriented  
313 intercalation of a cationic metal complex into layered silicates modified with  
314 organosulfonic-acid moieties. *Langmuir* 34, 4762–4773.

315 Takahashi, N., Kuroda, K., 2011. Materials design of layered silicates through covalent  
316 modification of interlayer surfaces. *J. Mater. Chem.* 21, 14336–14353.

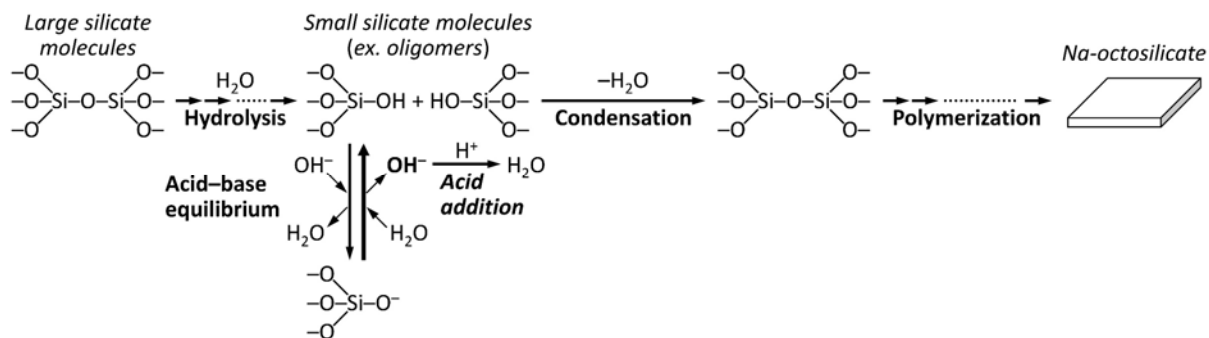
317 Vortmann, S., Rius, J., Siegmann, S., Gies, H., 1997. Ab initio structure solution from X-ray  
318 powder data at moderate resolution: crystal structure of a microporous layer silicate. *J. Phys.*  
319 *Chem. B* 101, 1292–1297.

320 Wang, Q., Zhang, Y., Jia, S., Han, Y., Xu, J., Meng, C., 2019. Self-assembled intercalation of 8-  
321 hydroxyquinoline into metal ions exchanged magadiites via solid-solid reaction and their  
322 optical properties. *Appl. Clay Sci.* 174, 47–56.

323 Werthmann, U., Marler, B., Gies, H., 2000. Pyrrolidine silica sodalite and ethylamine silica  
324 sodalite – two new silica sodalite materials synthesized from different solid silica sources.  
325 *Micropor. Mesopor. Mat.* 39, 549–562.

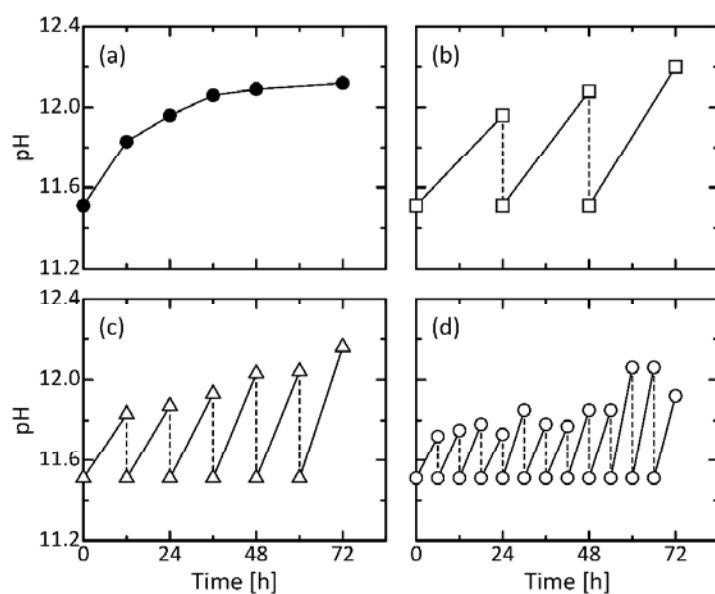
326 Yuan, Z., Tao, W., Wang, Z., Yang, W., 2019. One-step synthesis of highly dispersed nanosheets  
327 of magadiite. *Appl. Clay Sci.* 181, 105231.

328



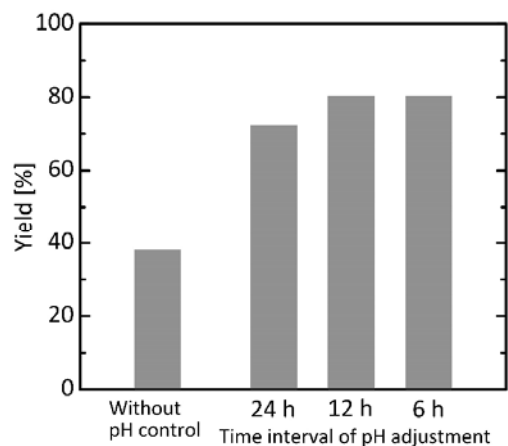
329  
330  
331  
332

**Scheme 1.** Possible reaction mechanism of the formation of Na-octosilicate.



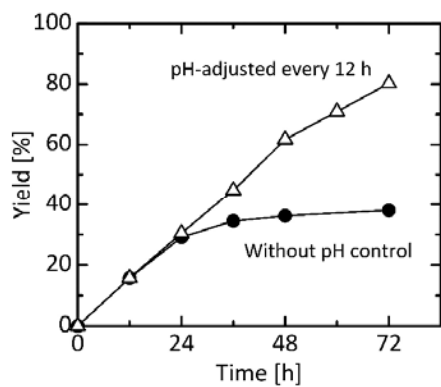
333  
334  
335  
336  
337

**Fig. 1.** Variation in pH with hydrothermal treatment time (a) without pH control and (b–d) with pH control using various time intervals of pH adjustment: (b) 24 h, (c) 12 h and (d) 6 h.



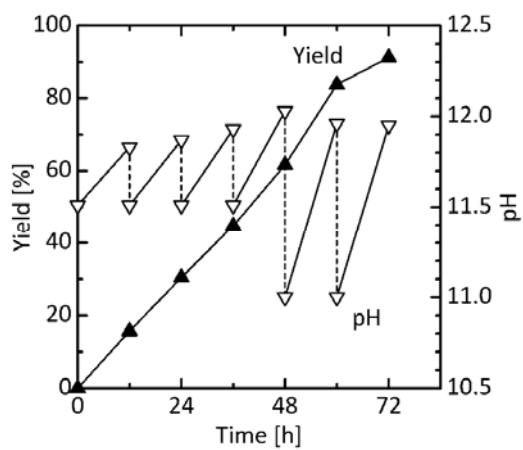
338  
339

**Fig. 2.** Yields in 72 h of hydrothermal treatment time with/without pH control.



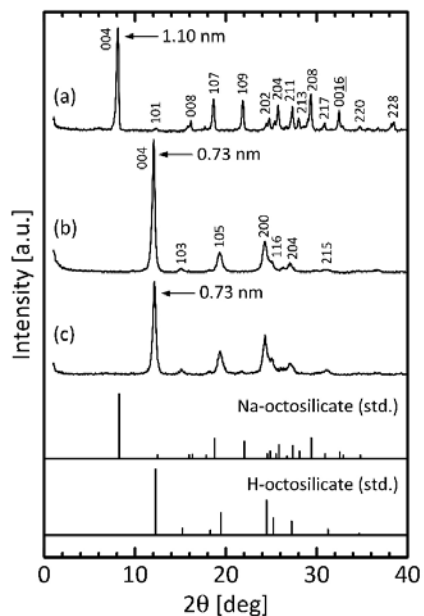
340  
 341 **Fig. 3.** Variations in yield with hydrothermal treatment time with/without pH control every 12  
 342 h of pH adjustment.

343  
 344



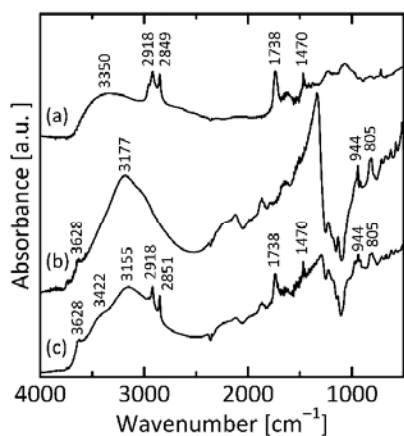
345  
 346 **Fig. 4.** Variation in pH and yield with hydrothermal treatment time using a specific pH  
 347 adjustment procedure.

348

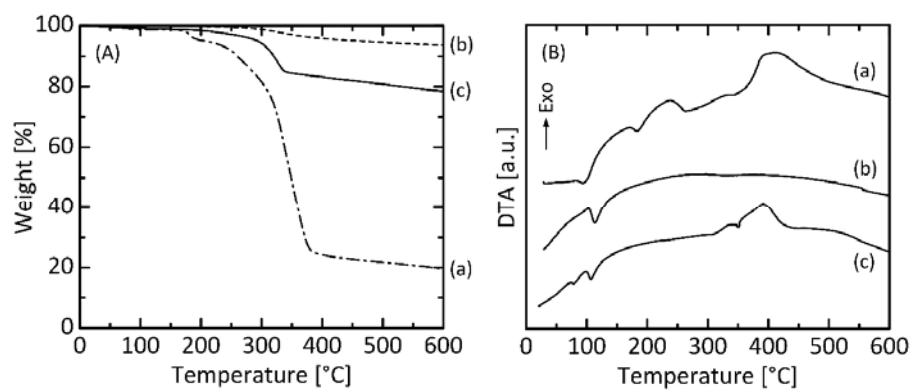


349  
 350 **Fig. 5.** XRD patterns of the samples obtained at each step after the pH-controlled hydrothermal  
 351 process using a specific pH adjustment procedure: (a) Na-octosilicate, (b) bare H-octosilicate  
 352 and (c) lecithin-coated H-octosilicate. The standard data of Na- and H-octosilicate were  
 353 obtained from the corresponding XRD patterns ranging from 5° to 35° in literature (Werthmann  
 354 et al., 2000).

355  
 356

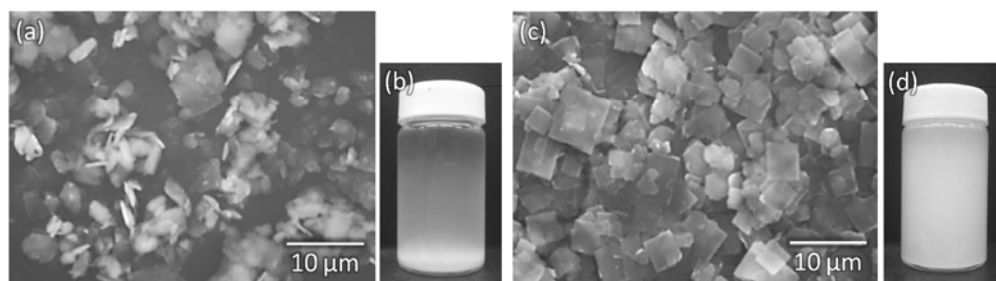


357  
 358 **Fig. 6.** IR spectra of (a) lecithin, (b) bare H-octosilicate and (c) lecithin-coated H-octosilicate.



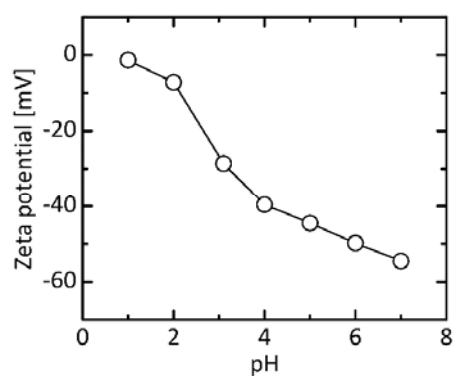
359  
 360 **Fig. 7.** (A) TG and (B) DTA curves of (a) lecithin, (b) bare H-octosilicate and (c) lecithin-coated  
 361 H-octosilicate.

362  
 363



364  
 365 **Fig. 8.** (a, c) SEM images of the dried samples and (b, d) photographs of the suspensions: (a,  
 366 b) bare, (c, d) lecithin-coated H-octosilicate.

367  
 368



369  
 370 **Fig. 9.** pH dependence of the zeta potential of a lecithin-coated H-octosilicate suspension.

371